

# Effects of Subunit I Mutations on Redox-Linked Conformational Changes of the *Escherichia coli* *bo*-type Ubiquinol Oxidase Revealed by Fourier-Transform Infrared Spectroscopy<sup>1</sup>

Yoichi Yamazaki,\* Hideki Kandori,\*<sup>2</sup> and Tatsushi Mogi<sup>†</sup>

\*Department of Biophysics, Graduate School of Science, Kyoto University, Sakyo-ku, Kyoto 606-8502; and

<sup>†</sup>Department of Biological Sciences, Graduate School of Science, The University of Tokyo, Hongo, Bunkyo-ku, Tokyo 113-0033

Received March 25, 1999; accepted May 6, 1999

Cytochrome *bo* is the heme-copper terminal ubiquinol oxidase in the aerobic respiratory chain of *Escherichia coli*, and functions as a redox-coupled proton pump. As an extension to our mutagenesis and Fourier-transform infrared studies on ion pumps, we examined the effects of subunit I mutations on redox-linked protein structural changes in cytochrome *bo*. Upon photo-reduction in the presence of riboflavin, Y288F and H333A showed profound effects in their peptide backbone vibrations (amide-I and amide-II), probably due to the loss of Cu<sub>B</sub> or replacement of high-spin heme *o* with heme B. In the frequency region of protonated carboxylic C=O stretching vibrations, negative 1,743 cm<sup>-1</sup> and positive 1,720 cm<sup>-1</sup> bands were observed in the wild-type; the former shifted to 1,741 cm<sup>-1</sup> in E286D but not in other mutants including D135N. This suggests that Glu286 in the D-channel is protonated in the air-oxidized state and undergoes hydrogen bonding changes upon reduction of the redox metal centers. Two pairs of band shifts at 2,566 (+)/2,574 (-) and 2,546 (+)/2,556 (-) cm<sup>-1</sup> in all mutants indicate that two cysteine residues not in the vicinity of the metal centers undergo redox-linked hydrogen bonding changes. Cyanide had no effect on the protein structural changes because of the rigid local protein structure around the binuclear center or the presence of a ligand(s) at the binuclear center, and was released from the binuclear center upon reduction. This study establishes that cytochrome *bo* undergoes unique redox-linked protein structural changes. Localization and time-resolved analysis of the structural changes during dioxygen reduction will facilitate understanding of the molecular mechanism of redox-coupled proton pumping at the atomic level.

**Key words:** FTIR, ubiquinol oxidase, cytochrome *bo*, redox difference spectra, protein backbone change.

Cytochrome *bo* is a four-subunit ubiquinol oxidase in the aerobic respiratory chain of *Escherichia coli* and is predominantly expressed under highly aerated growth conditions (1, 2 for reviews). It catalyzes the two-electron oxidation of ubiquinol-8 at the periplasmic side of the cytoplasmic membrane and the four-electron reduction of dioxygen at the cytoplasmic side. Accordingly, four scalar (or chemical) protons are apparently translocated from the cytoplasm to

the periplasm, generating an electrochemical proton gradient across the membrane. In addition, cytochrome *bo* can vectorially translocate four other protons per dioxygen reduction by a pump mechanism.

Subunit I binds all the redox metal centers, low-spin heme *b*, high-spin heme *o*, and Cu<sub>B</sub>, and the heme *o*-Cu<sub>B</sub> binuclear center serves as a reaction center for dioxygen reduction (1, 2). Mutagenesis and X-ray crystallographic studies on heme-copper terminal oxidases suggest that the D- and K-channels in subunit I are operative in redox-coupled proton pumping (3, 4). Photoaffinity cross-linking (5, 6) and mutagenesis studies (7, 8) have shown that the low-affinity quinol-oxidation site (QL) (9) resides in the C-terminal hydrophilic domain of subunit II. The high-affinity quinone binding site (QH) mediates intramolecular electron transfer between QL and heme *b* (10–13). Subunits III and IV are not involved in catalytic functions but are required for assembly of the redox metal centers in subunit I (14–16).

Our previous site-directed mutagenesis studies on the conserved residues in subunit I showed that not only metal ligand histidines (17–19) but also other charged amino acid

<sup>1</sup> This work was supported in part by Grants-in-Aid for Scientific Research on Priority Areas (10129215 and 10206206 to HK, 08249106 and 09257213 to TM) and for Scientific Research (A) (10358016 to HK) and (B) (08458202 to TM) from the Ministry of Education, Science, Sports and Culture of Japan. YY is supported by a research fellowship from the Japan Society for the Promotion of Science for young scientists. This is paper XXXVI in the series "Structure-function studies on the *E. coli* cytochrome *bo*."

<sup>2</sup> To whom correspondence should be addressed. Fax: +81-75-753-4210, E-mail: kandori@photo2.biophys.kyoto-u.ac.jp  
Abbreviations: FTIR, Fourier-transform infrared; QH, the high-affinity quinone binding site; QL, the low-affinity quinol oxidation site.

residues in the putative proton channels (20, 21) are crucial for the assembly of the redox metal centers. They are likely to be involved in the vectorial translocation of pumped and/or chemical protons (3, 4, 22–24); thus an examination of changes in the protonation and hydrogen bonding states of the conserved charged amino residues is essential for understanding the pathways and sequences of proton translocation across the oxidase protein. In addition, the redox metal centers must play an important role in redox-linked protein structural changes to drive the dioxygen reduction cycle and proton pumping mechanism.

Fourier-transform infrared (FTIR) spectroscopy has been used to probe the molecular environment of the active center of terminal oxidases using respiratory inhibitors such as CO and cyanide (25, 26). Recently, the application of a spectro-electrochemical cell (27, 28) and the introduction of photo-activatable electron donors (29–31) enabled us to examine protein structural changes that occur upon reduction of the redox metal centers of respiratory terminal oxidases. Alternatively, the photodissociation of CO from reduced cytochrome *bo* at 80 K revealed local structural changes surrounding the heme-copper binuclear center (32).

In the present article, we applied the method of Lübben and Gerwert (29) to *E. coli* cytochrome *bo* and examined the effects of subunit I mutations and cyanide binding on redox-linked protein structural changes by FTIR spectroscopy. Asp135Asn, Glu286Asp, and Glu286Gln (20) could identify structural changes in the carboxylic side-chains at Asp135 and Glu286 in the D-channel when the protonated carboxylic CO-stretching vibrations were monitored, and Tyr288Phe (20) and His333Ala (17) could probe the possible roles of Cu<sub>B</sub> and high-spin heme *o* in redox-linked protein structural changes in the amide-I and -II regions, and the protonated carboxylic CO- and cysteine SH-stretching vibration regions.

#### MATERIALS AND METHODS

**Purification of Cytochrome *bo***—Wild-type and His333-Ala mutant enzymes were isolated from the overproducing strains GO103/pHN3795-1 (*cyo*+*Δcyd*/*cyo*+Apr) and ST4533/pHN3795-H333A (*Δcyo cyd*+/*cyo*-Apr), respectively, as described previously (26, 33). Asp135Asn, Glu286Asp, Glu286Gln, and Tyr288Phe were purified from ST4676 (*Δcyo cyd*) harboring the derivatives of a single copy plasmid pMFO9 (*cyo*+ -Apr) (20, 34).

**FTIR and Visible Spectroscopies**—Spectroscopic analyses were carried out as described previously (31). Photo-reduction of the air-oxidized enzymes was conducted at room temperature (25°C) in the presence of riboflavin as a photoactivatable electron donor (29).

#### RESULTS AND DISCUSSION

**Visible Absorption Changes upon Photoreduction**—Photo-reduced *minus* air-oxidized redox difference spectra (Fig. 1) indicate that 2 min illumination in the presence of riboflavin results in the reduction of both low-spin and high-spin hemes of subunit I mutants except Glu286Gln to a level similar to the wild-type enzyme (88%). It was quite difficult to reduce Glu286Gln under the present conditions. During illumination, dissolved dioxygen in the sample must

be exhausted by repeated turnover of the oxidase reaction. Redox difference spectra of the wild-type, Asp135Asn, and Glu286Asp enzymes show absorption maxima at 428, 529, and 561 nm, characteristic of the fully reduced cytochrome *bo*. It should be noted that due to the replacement of heme O at the high-spin heme binding site with heme B (20, 21), the Soret peak of air-oxidized Tyr288Phe shifted from 408 nm as seen in the wild-type to 413 nm (data not shown), and a trough in the difference spectrum shifted from 400 to 409 nm (Fig. 1). In contrast, other mutants showed only slight changes in the Soret region.

**Infrared Spectral Changes in the 1,800–1,300 cm<sup>-1</sup> Region**—Photo-reduced *minus* air-oxidized FTIR difference spectra of Asp135Asn and Glu286Asp are similar to that of the wild-type which shows positive bands at 1,663, 1,653, and 1,635 cm<sup>-1</sup> (Fig. 2, a–c), frequencies typical of α<sub>11</sub>-helix, α<sub>1</sub>-helix, and β-sheet structures, respectively (35). In contrast, marked differences were observed in the amide-I region (1,700–1,600 cm<sup>-1</sup>) of Tyr288Phe and His333Ala (Fig. 2, d and e). The positive 1,653-cm<sup>-1</sup> band is almost absent in His333Ala, while a sharp negative peak is present at 1,668 cm<sup>-1</sup> in Tyr288Phe and His333Ala. Regular (α<sub>1</sub>-helix) and distorted (α<sub>11</sub>-helix) helices possess amide-I frequencies at 1,650–1,660 cm<sup>-1</sup> and 1,660–1,670 cm<sup>-1</sup>, respectively (35). The results on Tyr288Phe and His333Ala thus imply an alteration in the local protein structure around the heme *o*-Cu<sub>B</sub> binuclear center, particularly in the helices. In the amide-II region, two positive peaks at 1,545 and 1,537 cm<sup>-1</sup> in the wild-type, frequencies

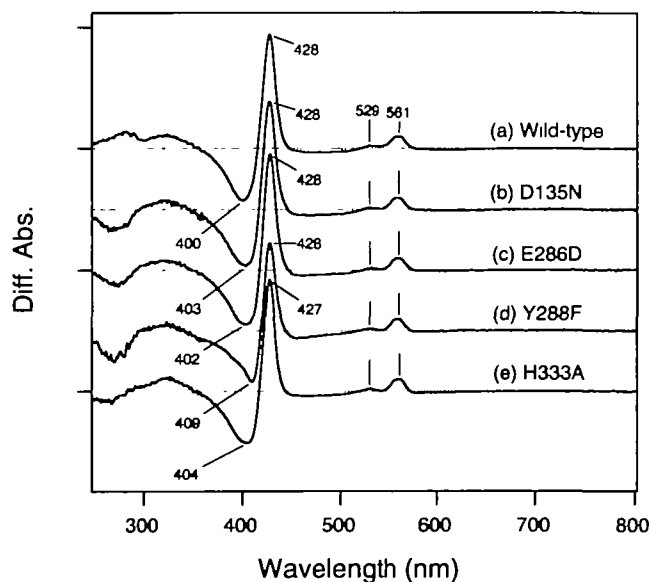


Fig. 1. Photo-reduced *minus* air-oxidized visible absorption difference spectra of subunit I mutants of cytochrome *bo*. Five microliters of enzyme (wild-type, 0.275 mM; D135N, 0.12 mM; E286D, 0.15 mM; Y288F, 0.09 mM; H333A, 0.24 mM) in 50 mM Tris-HCl (pH 7.4) containing 0.1% sucrose monolaurate (Mitsubishi-Kagaku Foods, Tokyo), 0.25 mM riboflavin, and 50 mM sodium EDTA was partially dehydrated *in vacuo* on a BaF<sub>2</sub> window, and covered with another window with a 6-mm diameter aperture (31). Spectra were obtained at room temperature (25°C) with a dispersive Shimadzu MPS-2000 spectrometer before and after 2 min illumination with a tungsten-halogen lamp (31). Spectral changes were normalized to the absorbance at 560 nm of the wild-type enzyme. One division of the Y-axis corresponds to 0.2 absorbance unit.

typical of  $\alpha$ -helices, are preserved in Asp135Asn and Glu286Asp (Fig. 2, a-c). A slight shift in the positive 1,537-cm<sup>-1</sup> band to 1,540 cm<sup>-1</sup> in Tyr288Phe and its absence in His333Ala provide further support for structural perturbations of helices in these two mutants.

His284 and Tyr288 are both present in helix VI (36) where a regular  $\alpha$ -helical structure is perturbed by Pro285 (2, 4). Tyr288Phe undergoes loss of the Cu<sub>B</sub> (20) that is ligated to His284, His333, and His334 (17-19, 37, 38), a covalent bond between Tyr288 and His284 (39, 40), and a hydrogen bond between the OH group of Tyr288 and the OH group of hydroxyethylfarnesyl chain of the high-spin heme *o* (41) due to replacement with heme B (20). Accordingly, Tyr288Phe causes a direct alteration of the  $\alpha$ -helical structure of helix VI and also that of helix X through His419, the high-spin heme ligand (18, 19, 42).

His333 and His334 are located in loop VII/VIII (4, 39, 41) and the imidazole ring of His333 can adopt two alternative conformations upon ligand binding to the binuclear center (4). His333Ala lacks Cu<sub>B</sub> completely but has no significant effect on the bound hemes (17, 33). Thus His333Ala is unlikely to affect helices VII and X but might alter the structure of helix VI through His284, which has lost the bound Cu<sub>B</sub>. In conclusion, binuclear center mutations have large effects on redox-linked protein structural changes brought about by the loss and/or substitution of metal centers.

In the protonated carboxylic C=O stretching region, the wild-type enzyme shows a redox-linked hydrogen-bonding change from 1,743 cm<sup>-1</sup> to 1,720 cm<sup>-1</sup> that is attributable to one Asp or Glu residue (Fig. 3, dotted line). The frequency of the oxidized form is comparable to previous

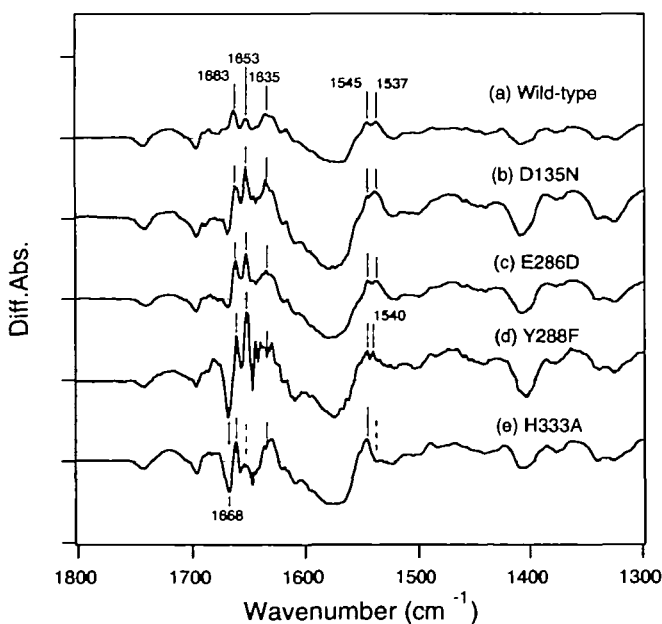


Fig. 2. Photo-reduced *minus* air-oxidized infrared difference spectra of subunit I mutants in the amide-I and amide-II (1,800-1,300 cm<sup>-1</sup>) region. Two hundred fifty-six interferograms at 2 cm<sup>-1</sup> resolution were recorded at room temperature (25°C) with a Bio-Rad FTS-40 FTIR spectrometer (31). One division of the Y-axis corresponds to 0.004 absorbance unit. Other details are the same as in the legend to Fig. 1.

reports (1,745 cm<sup>-1</sup>), whereas that of the reduced form is considerably different from the 1,735 cm<sup>-1</sup> reported by Lübben and coworkers (29, 30). Changes were also observed in Asp135Asn, Tyr288Phe, and His333Ala, however, a negative peak in air-oxidized Glu286Asp clearly shifted to 1,741 cm<sup>-1</sup> with reduced intensity. It is thus concluded that this band contains the C=O stretching vibration of Glu286. The effect of Glu286 mutations on infrared changes is consistent with our recent report that such mutations affect the binuclear center structure of the air-oxidized form (34). In general, the protonated carboxylic C=O stretch appears in the 1,700-1,780 cm<sup>-1</sup> region, and the frequency shifts lower if the hydrogen bonding is strengthened. The frequency shift from 1,743 cm<sup>-1</sup> to 1,720 cm<sup>-1</sup> originates from the strengthened hydrogen bonding of Glu286 upon the reduction of metalcenters.

Hellwig *et al.* showed that redox-induced infrared changes at 1,746(-) and 1,734(+) cm<sup>-1</sup> in *aa3*-type cytochrome *c* oxidase from *Paracoccus denitrificans* were associated with electron transfer from/to low-spin heme *a* and disappeared in Glu278Gln and Glu278Asp but were unaffected in Asp124Asn and Asp399Asn (28). During the revision of this manuscript, Lübben *et al.* reported that the 1,745/1,735 cm<sup>-1</sup> signals were lost in Glu286Asp and Glu286Gln mutants of *E. coli* cytochrome *bo* but retained in Asp135Glu and Asp407Asn mutants (30). For an unknown reason, they were unable to express enough Asp135Asn for purification. Although the discrepancy in the frequencies reported in this study and that of Lübben *et al.* (30) remains to be explained, it can be concluded that the side-chain of the conserved Glu residue in the middle of helix VI is protonated in the air-oxidized state and undergoes a hydrogen bonding change upon reduction of the metal centers, because a membrane-buried carboxylic residue is

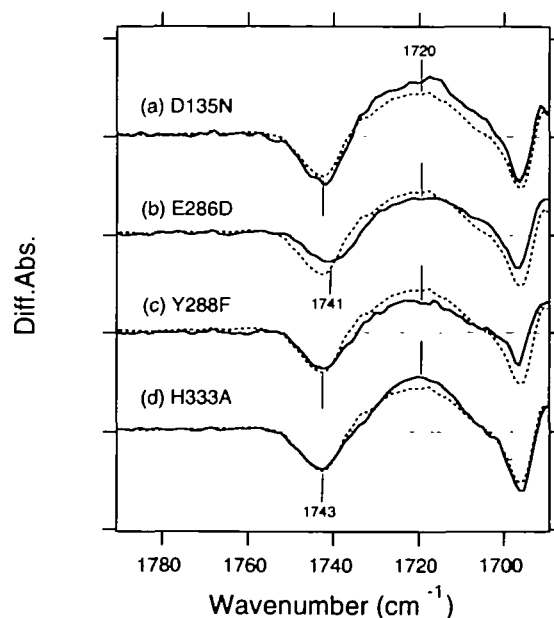


Fig. 3. Photo-reduced *minus* air-oxidized infrared difference spectra of subunit I mutants in the protonated CO stretching frequency region. The dotted line in each panel indicates the wild-type enzyme. One division of the Y-axis corresponds to 0.001 absorbance unit. Other details are the same as in the legend to Fig. 2.

expected to be protonated (4), and the frequencies of this band pair in fact show a downshift when the solvent is changed to D<sub>2</sub>O (27–30). It should be noted that mutations at the heme-copper binuclear center (Tyr288Phe and His333Ala) and at the ends of the proton channel (Asp135Asn, Asp135Glu, and Asp407Asn) do not affect the redox-induced protein structural changes at Glu286.

Thus FTIR spectroscopy is demonstrated to be a powerful tool with which to probe the protonation and hydrogen bonding states of carboxylic residues in the proton channel, since X-ray crystallographic studies on cytochrome *c* oxidases fail to detect such a redox-induced microenvironmental change (4, 39–41). Upon reduction of the metal centers, two chemical protons are delivered to the heme-copper binuclear center through the K-channel to compensate for the two additional negative charges (3, 43). However, the side-chain of Glu286 is located on the side opposite to His284, which ligates Cu<sub>B</sub> at the end of the K-channel, and protrudes into the D-channel. Redox-linked hydrogen bonding changes at Glu286 cannot be involved in the translocation of the initial two chemical protons, but may be related to the proton release to the periplasm through the D-channel during subsequent steps of dioxygen reduction (3, 44).

**Infrared Spectral Changes in the SH Stretching Region**—We were able to extend infrared studies on redox-linked protein structural changes of terminal oxidases (27–30) to 2,620 cm<sup>-1</sup> (31). Upon hydrogen bonding change, the SH stretching vibration of cysteine residues show a small frequency shift in the 2,580–2,525 cm<sup>-1</sup> region (45–47). We found two positive and negative peaks at 2,566 and 2,546 cm<sup>-1</sup>, and 2,574 and 2,556 cm<sup>-1</sup>, respectively, in the wild-type and mutant enzymes other than Tyr288Phe (Fig. 4). This indicates that one SH group corresponding to the

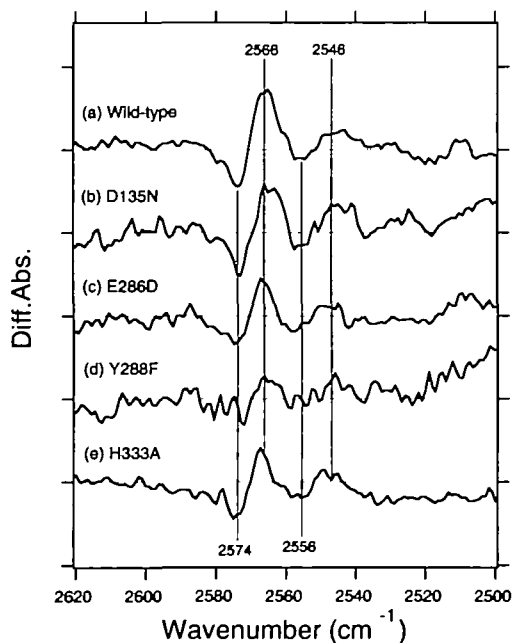


Fig. 4. Photo-reduced *minus* air-oxidized infrared difference spectra of subunit I mutants in the cysteine SH stretching frequency (2,620–2,500 cm<sup>-1</sup>) region. One division of the Y-axis corresponds to 0.0001 absorbance unit. Other details are the same as in the legend to Fig. 2.

2,574 cm<sup>-1</sup> band forms a new hydrogen bond upon reduction (46, 47), and that the other corresponding to the 2,556 cm<sup>-1</sup> band undergoes stronger hydrogen bonding. The large decrease in the signal intensity for Tyr288Phe may be related to the replacement of heme O at the high-spin heme binding site (20), a lack of a covalent bond between the side chains of Tyr288 and His284 (39, 40), or a direct proton donor to the binuclear center (3, 40).

Subunit I of cytochrome *bo* binds all the redox metal centers (17–19, 37, 38, 42) and contains four cysteines at the cytoplasmic end of helices V (Cys234), X (Cys432), and XII (Cys511) and the middle of helix VII (Cys322) (36). Although all these residues are functionally dispensable (32), redox-linked changes in the cysteine SH stretching vibrations may represent protein structural changes associated with the opening of the proton channel(s) or the delivery of two chemical protons (3, 43). These results indicate that at least two cysteines undergo hydrogen bonding changes between the oxidized and reduced states, and that they are not located in the vicinity of the binuclear center. The assignment of such cysteine residues by site-directed mutagenesis will lead to a better understanding of redox-linked protein structural changes in cytochrome *bo*.

**Infrared Spectral Changes in the CN Stretching Region**—To localize redox-linked protein structural changes, the effect of cyanide binding to the binuclear metal center was examined. The air-oxidized wild-type enzyme exhibits an absorption maximum at 414 nm in the presence of KCN, and 92% of the cyanide-inhibited enzyme is photo-reduced upon 2 min illumination resulting in absorption maxima identical to those of the control enzyme. In the 2,180–2,025 cm<sup>-1</sup> region of the photo-reduced *minus* air-oxidized FTIR difference spectrum, we found a negative band at 2,146 cm<sup>-1</sup> assignable to the CN stretching vibration of the Fe<sup>3+</sup>-C=N-Cu<sub>B</sub><sup>2+</sup> bridging structure (26) and a positive band at 2,080 cm<sup>-1</sup> with a broad shoulder on the higher frequency side (Fig. 5). It has been reported that free HCN and CN<sup>-</sup> (deprotonated form) have CN stretching vibrations at

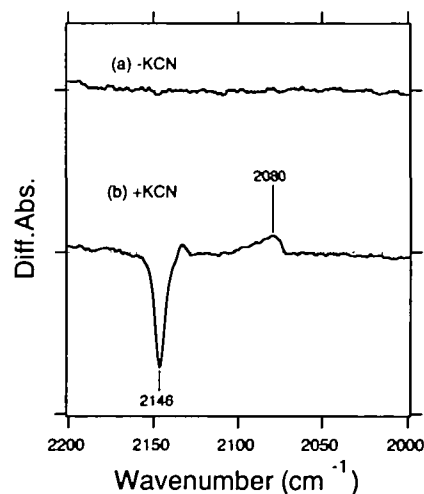


Fig. 5. Photo-reduced *minus* air-oxidized infrared difference spectra of wild-type cytochrome *bo* in the CN stretching frequency (2,200–2,000 cm<sup>-1</sup>) region. Potassium cyanide was added to the enzyme solution at 1.4 mM. One division of the Y-axis corresponds to 0.0005 absorbance unit. Other details are the same as in the legend to Fig. 2.

2,093 and 2,079  $\text{cm}^{-1}$ , respectively (48). Thus, the bound cyanide was released from the heme-copper binuclear center upon reduction of the binuclear metal center. This is consistent with the fact that the reduced form has the same visible absorption spectrum regardless of the presence or absence of cyanide. The concentration of cyanide in the sample (*i.e.*, 1.4 mM before partial dehydration) is much larger than the  $K_i$  value (0.01 mM) for ubiquinol-1 oxidation (49), but not enough to hold cyanide on the reduced high-spin heme *o* as on the oxidized form, because the  $K_d$  value for the reduced form is 7 (50) or 12 mM (M. Tsubaki, personal communication). The  $K_d$  value for the reduced form is different from those of *aa3*-type cytochrome *c* oxidase and *ba3*-type ubiquinol oxidase [ $K_d$ , 0.1–0.55 mM (51)] where the heme *a3*-Cu<sub>B</sub> center serves as the ligand binding site.

This study reveals that cyanide bound to the binuclear center does not affect redox-linked changes in the amide-I and -II regions, the protonated carboxylic C=O and cysteine SH stretching vibrations before and after photoreduction (data not shown). The binuclear center appears to contain a ligand in the air-oxidized state, perhaps a water molecule and a hydroxyl ion (38) or a peroxide (40) as found in the crystal structures of cytochrome *c* oxidases. Alternatively, the protein structure around the binuclear center is so rigid that cyanide binding does not affect the redox-linked protein structural changes.

The molecular mechanism of vectorial proton translocation has been studied extensively for light-driven proton pump bacteriorhodopsin by site-directed mutagenesis (52) and FTIR spectroscopy (53–55). We extended our mutagenesis and FTIR studies on ion pumps, and found that hydrogen bonding changes at Glu286 and protein backbone changes around the metal centers are associated with reduction of the metal centers of *E. coli* cytochrome *bo*. We recently found that similar redox-linked protein structural changes take place in cytochrome *bd* (31), an alternative ubiquinol oxidase, under microaerobic growth conditions, although it cannot pump protons (1). Therefore, systematic site-directed mutagenesis to localize such changes and time-resolved FTIR studies during dioxygen reduction are essential for understanding the molecular mechanism of the vectorial translocation of chemical and pumped protons in heme-copper terminal oxidases.

We thank R.B. Gennis (University of Illinois, Urbana) for the *E. coli* strain GO103 and M. Tsubaki (Himeji Institute of Technology) for personal communication.

#### REFERENCES

- Mogi, T., Tsubaki, M., Hori, H., Miyoshi, H., Nakamura, H., and Anraku, Y. (1998) Two terminal quinol oxidase families in *Escherichia coli*: Variations on molecular machinery for dioxygen reduction. *J. Biochem. Mol. Biol. Biophys.* **2**, 79–110
- Mogi, T., Nakamura, H., and Anraku, Y. (1994) Molecular structure of a heme-copper redox center of the *Escherichia coli* ubiquinol oxidase: Evidence and model. *J. Biochem.* **116**, 741–747
- Gennis, R.B. (1998) Multiple proton-conducting pathways in cytochrome oxidase and a proposed role for the active-site tyrosine. *Biochim. Biophys. Acta* **1365**, 241–248
- Iwata, S., Ostermeier, C., Ludwig, B., and Michel, H. (1995) Structure at 2.8 Å resolution of cytochrome *c* oxidase from *Paracoccus denitrificans*. *Nature* **376**, 660–669
- Welter, R., Gu, L.-Q., Yu, L., Yu, C.-A., Rumbley, J., and Gennis, R.B. (1994) Identification of the ubiquinol-binding site in the cytochrome *bo3*-ubiquinol oxidase of *Escherichia coli*. *J. Biol. Chem.* **269**, 28834–28838
- Tsatsos, P.H., Reynolds, K., Nickels, E.F., He, D.-Y., Yu, C.-A., and Gennis, R.B. (1998) Using matrix-assisted laser desorption/ionization mass spectroscopy to map the quinol binding site of cytochrome *bo3* from *Escherichia coli*. *Biochemistry* **37**, 9884–9888
- Ma, J., Puustinen, A., Wikström, M., and Gennis, R.B. (1998) Tryptophan-136 in subunit II of cytochrome *bo3* from *Escherichia coli* may participate in the binding of ubiquinol. *Biochemistry* **37**, 11806–11811
- Sato-Watanabe, M., Mogi, T., Miyoshi, H., and Anraku, Y. (1998) Isolation and characterizations of quinone analogue-resistant mutants of *bo*-type ubiquinol oxidase from *Escherichia coli*. *Biochemistry* **37**, 12744–12752
- Sato-Watanabe, M., Mogi, T., Miyoshi, H., Iwamura, H., Matsushita, K., Adachi, O., and Anraku, Y. (1994) Structure-function studies on the ubiquinol oxidation site of the cytochrome *bo* complex from *Escherichia coli* using *p*-benzoquinones and substituted phenols. *J. Biol. Chem.* **269**, 28899–28907
- Sato-Watanabe, M., Mogi, T., Ogura, T., Kitagawa, T., Miyoshi, H., Iwamura, H., and Anraku, Y. (1994) Identification of a novel quinone binding site in the cytochrome *bo* complex from *Escherichia coli*. *J. Biol. Chem.* **269**, 20908–20912
- Sato-Watanabe, M., Itoh, S., Mogi, T., Matsuura, K., Miyoshi, H., and Anraku, Y. (1995) Stabilization of a semiquinone radical at the high affinity quinone binding site of the *Escherichia coli bo*-type ubiquinol oxidase. *FEBS Lett.* **374**, 265–269
- Sato-Watanabe, M., Mogi, T., Miyoshi, H., and Anraku, Y. (1998) Characterization and functional role of the QH site of *bo*-type quinol oxidase from *Escherichia coli*. *Biochemistry* **37**, 5356–5361
- Ingledew, W.J., Ohnishi, T., and Salerno, J.C. (1995) Studies on a stabilization of ubisemiquinone by *Escherichia coli* quinol oxidase, cytochrome *bo*. *Eur. J. Biochem.* **227**, 903–908
- Nakamura, H., Saiki, K., Mogi, T., and Anraku, Y. (1997) Assignment and functional roles of the *cyoABCDE* gene products required for the *Escherichia coli bo*-type ubiquinol oxidase. *J. Biochem.* **122**, 415–421
- Saiki, K., Mogi, T., and Anraku, Y. (1996) Probing a role of subunit IV of the *Escherichia coli bo*-type ubiquinol oxidase by deletion and cross-linking analyses. *J. Biol. Chem.* **271**, 15336–15340
- Saiki, K., Mogi, T., Tsubaki, M., Hori, H., and Anraku, Y. (1997) Exploring subunit-subunit interactions in the *Escherichia coli bo*-type ubiquinol oxidase by extragenic suppressor mutation analysis. *J. Biol. Chem.* **272**, 14721–14726
- Minagawa, J., Mogi, T., Gennis, R.B., and Anraku, Y. (1992) Identification of heme and copper ligands in subunit I of the cytochrome *bo* complex in *Escherichia coli*. *J. Biol. Chem.* **267**, 2096–2104
- Uno, T., Mogi, T., Tsubaki, M., Nishimura, Y., and Anraku, Y. (1994) Resonance Raman and Fourier-transform infrared studies on the subunit I histidine mutants of the cytochrome *bo* complex in *Escherichia coli*: Molecular structure of redox centers. *J. Biol. Chem.* **269**, 11912–11920
- Tsubaki, M., Mogi, T., Hori, H., Ogura, T., Hirota, S., Kitagawa, T., and Anraku, Y. (1994) Molecular structure of redox metal centers of the cytochrome *bo* complex from *Escherichia coli*: Spectroscopic characterizations of the subunit I histidine mutant oxidases. *J. Biol. Chem.* **269**, 30861–30868
- Kawasaki, M., Mogi, T., and Anraku, Y. (1997) Substitutions of charged amino acid residues conserved in subunit I perturb the redox metal centers of the *Escherichia coli bo*-type ubiquinol oxidase. *J. Biochem.* **122**, 422–429
- Mogi, T., Minagawa, J., Hirano, T., Sato-Watanabe, M., Tsubaki, M., Uno, T., Hori, H., Nakamura, H., Nishimura, Y., and Anraku, Y. (1998) Substitutions of conserved aromatic amino acid residues in subunit I perturb the metal centers of the *Escherichia coli bo*-type ubiquinol oxidase. *Biochemistry* **37**, 1632–1639
- Thomas, J.W., Puustinen, A., Alben, J.O., Gennis, R.B., and Wikström, M. (1993) Substitution of asparagine for aspartate-135 in subunit I of the cytochrome *bo* ubiquinol oxidase of

- Escherichia coli* eliminates proton-pumping activity. *Biochemistry* **32**, 10923-10928
23. Verkhovskaya, M.L., Garcia-Horsman, A., Puustinen, A., Rigaud, J.L., Morgan, J.E., Verkhovsky, M.I., and Wikström, M. (1997) Glutamic acid 286 in subunit I of cytochrome *bo3* is involved in proton translocation. *Proc. Natl. Acad. Sci. USA* **94**, 10128-10131
  24. Konstantinov, A.A., Siletsky, S., Mitchell, D., Kaulen, A., and Gennis, R.B. (1997) The roles of two proton input channels in cytochrome *c* oxidase from *Rhodobacter sphaeroides* probed by the effects of site-directed mutations on time-resolved electrogenic intraprotein proton transfer. *Proc. Natl. Acad. Sci. USA* **94**, 9085-9090
  25. Alben, J.O., Moh, P.P., Fiamingo, F.G., and Altschuld, R.A. (1981) Cytochrome oxidase (*a3*) heme and copper observed by low-temperature Fourier transform infrared spectroscopy of the CO complex. *Proc. Natl. Acad. Sci. USA* **78**, 234-237
  26. Tsubaki, M., Mogi, T., Anraku, Y., and Hori, H. (1993) Structure of the heme-copper binuclear center of the cytochrome *bo* complex of *Escherichia coli*: EPR and Fourier transform infrared spectroscopic studies. *Biochemistry* **32**, 6065-6072
  27. Hellwig, P., Rost, B., Kaiser, U., Ostermeier, C., Michel, H., and Mantele, W. (1996) Carboxyl group protonation upon reduction of the *Paracoccus denitrificans* cytochrome *c* oxidase: Direct evidence by FTIR spectroscopy. *FEBS Lett.* **385**, 53-57
  28. Hellwig, P., Behr, J., Ostermeier, C., Richter, O.-M.H., Pftzner, U., Odenwald, A., Ludwig, B., Michel, H., and Mantele, W. (1998) Involvement of glutamic acid 278 in the redox reaction of the cytochrome *c* oxidase from *Paracoccus denitrificans* investigated by FTIR spectroscopy. *Biochemistry* **37**, 7390-7399
  29. Lübben, M. and Gerwert, K. (1996) Redox FTIR difference spectroscopy using caged electrons reveals contribution of carboxyl groups to catalytic mechanism of haem-copper oxidases. *FEBS Lett.* **397**, 303-307
  30. Lübben, M., Prutsch, A., Mamat, B., and Gerwert, K. (1999) Electron transfer induces side-chain conformational changes of glutamate-286 from cytochrome *bo*. *Biochemistry* **38**, 2048-2056
  31. Yamazaki, Y., Kandori, H., and Mogi, T. (1999) Fourier-transform infrared studies on conformational changes of *bd*-type ubiquinol oxidase from *Escherichia coli* upon photoreduction of the redox metal centers. *J. Biochem.* **125**, 1131-1136
  32. Puustinen, A., Bailey, J.A., Dyer, R.B., Mecklenburg, S.L., Wikström, M., and Woodruff, W.H. (1997) Fourier transform infrared evidence for connectivity between Cu<sub>2</sub> and glutamic acid 286 in cytochrome *bo3* from *Escherichia coli*. *Biochemistry* **36**, 13195-13200
  33. Mogi, T., Hirano, T., Nakamura, H., Anraku, Y., and Orii, Y. (1995) Cu<sub>2</sub> promotes both binding and reduction of dioxygen at the heme-copper binuclear center in the *Escherichia coli bo*-type ubiquinol oxidase. *FEBS Lett.* **370**, 259-263
  34. Tsubaki, M., Hori, H., and Mogi, T. (1997) Glutamate-286 mutants of cytochrome *bo*-type ubiquinol oxidase from *Escherichia coli*: Influence of mutations on the binuclear metal center structure revealed by FT-IR and EPR spectroscopies. *FEBS Lett.* **416**, 247-250
  35. Krimm, S. and Bandekar, J. (1986) Vibrational spectroscopy and conformation of peptides, polypeptides, and proteins. *Adv. Protein Chem.* **38**, 183-364
  36. Chepuri, V., Lemieux, L., Au, D.C.T., and Gennis, R.B. (1990) The sequence of the *cyo* operon indicates substantial structural similarities between the cytochrome *o* ubiquinol oxidase of *Escherichia coli* and the *aa3*-type family of cytochrome *c* oxidases. *J. Biol. Chem.* **265**, 11185-11192
  37. Lemieux, L.J., Calhoun, M.W., Thomas, J.W., Ingledew, W.J., and Gennis, R.B. (1992) Determination of the ligands of the low spin heme of the cytochrome *o* ubiquinol oxidase complex using site-directed mutagenesis. *J. Biol. Chem.* **267**, 2105-2113
  38. Calhoun, M.W., Hill, J.J., Lemieux, L.J., Ingledew, W.J., Alben, J.O., and Gennis, R.B. (1993) Site-directed mutants of the cytochrome *bo* ubiquinol oxidase of *Escherichia coli*: Amino acid substitutions for two histidines that are putative Cu<sub>2</sub> ligands. *Biochemistry* **32**, 11524-11529
  39. Ostermeier, C., Harrenga, A., Ermler, U., and Michel, H. (1997) Structure at 2.7 Å resolution of the *Paracoccus denitrificans* two-subunit cytochrome *c* oxidase complexed with an antibody FV fragment. *Proc. Natl. Acad. Sci. USA* **94**, 10547-10553
  40. Yoshikawa, S., Shinzawa-Itoh, K., Nakashima, R., Yaono, R., Yamashita, E., Inoue, N., Yao, M., Fei, M.J., Libei, C.P., Mizushima, T., Yamaguchi, H., Tomizaki, T., and Tsukihara, T. (1998) Redox-coupled crystal structural changes in bovine heart cytochrome *c* oxidase. *Science* **280**, 1723-1729
  41. Tsukihara, T., Aoyama, H., Yamashita, E., Tomizaki, T., Yamaguchi, H., Shinzawa-Itoh, K., Nakashima, R., Yaono, R., and Yoshikawa, S. (1996) The whole structure of the 13-subunit oxidized cytochrome *c* oxidase at 2.8 Å. *Science* **272**, 1136-1144
  42. Calhoun, M.W., Thomas, J.W., Hill, J.J., Hosler, J.P., Shapleigh, J.P., Tecklenburg, M.M.J., Ferguson-Miller, S., Babcock, G.T., Alben, J.O., and Gennis, R.B. (1993) Identity of the axial ligand of the high-spin heme in cytochrome oxidase: Spectroscopic characterization of mutants in the *bo*-type oxidase of *Escherichia coli* and the *aa3*-type oxidase of *Rhodobacter sphaeroides*. *Biochemistry* **32**, 10905-10911
  43. Karperfors, M., Adelroth, P., Aagaard, A., Sigurdson, H., Svensson-Ek, M., and Brzezinski, P. (1998) Electron-proton interactions in terminal oxidases. *Biochim. Biophys. Acta* **1365**, 159-169
  44. Babcock, G.T. and Wikström, M. (1992) Oxygen activation and the conservation of energy in cell respiration. *Nature* **356**, 301-309
  45. Alben, J.O., Bare, G.H., and Bromberg, P.A. (1974) Sulfhydryl groups as a new molecular probe at the alpha1 beta1 interface in haemoglobin using Fourier transform infrared spectroscopy. *Nature* **252**, 736-737
  46. Li, H. and Thomas, G.J. Jr. (1991) Cysteine conformation and sulfhydryl interaction in proteins and viruses. I. Correlation of the Raman S-H band with hydrogen bonding and intramolecular geometry in model compounds. *J. Am. Chem. Soc.* **113**, 456-462
  47. Kandori, H., Kinoshita, N., Shichida, Y., Maeda, A., Needleman, R., and Lanyi, J.K. (1998) Cysteine S-H as a hydrogen-bonding probe in proteins. *J. Am. Chem. Soc.* **120**, 5828-5829
  48. Tsubaki, M., Mogi, T., Hori, H., Sato-Watanabe, M., and Anraku, Y. (1996) Infrared and EPR studies on cyanide binding to the heme-copper binuclear center of cytochrome *bo*-type ubiquinol oxidase from *Escherichia coli*. Release of a Cu<sub>2</sub>-cyano complex in the partially reduced state. *J. Biol. Chem.* **271**, 4017-4022
  49. Kita, K., Konishi, K., and Anraku, Y. (1984) Terminal oxidases of *Escherichia coli* aerobic respiratory chain. II. Purification and properties of cytochrome *b558-d* complex from cells grown with limited oxygen and evidence of branched electron-carrying systems. *J. Biol. Chem.* **259**, 3375-3381
  50. Mitchell, R., Moody, A.J., and Rich, P.R. (1995) Cyanide and carbon monoxide binding to the reduced form of cytochrome *bo* from *Escherichia coli*. *Biochemistry* **34**, 7576-7585
  51. Tsubaki, M., Matsushita, K., Adachi, O., Hirota, S., Kitagawa, T., and Hori, H. (1997) Resonance Raman, infrared, and EPR investigation on the binuclear site structure of the heme-copper ubiquinol oxidases from *Acetobacter aceti*. Effect of the heme peripheral formyl group substitution. *Biochemistry* **36**, 13034-13042
  52. Mogi, T., Stern, L.J., Marti, T., Chao, B.H., and Khorana, H.G. (1988) Aspartic acid substitutions affect proton translocation by bacteriorhodopsin. *Proc. Natl. Acad. Sci. USA* **85**, 4148-4152
  53. Braiman, M.S., Mogi, T., Marti, T., Stern, L.J., Khorana, H.G., and Rothschild, K.J. (1988) Vibrational spectroscopy on bacteriorhodopsin mutants: Light-driven proton transport involves protonation changes of aspartic acid residues 85, 96, and 212. *Biochemistry* **27**, 8516-8520
  54. Yamazaki, Y., Tuzi, S., Saitō, H., Kandori, H., Needleman, R., Lanyi, J.K., and Maeda, A. (1996) Hydrogen bonds of water and C=O groups coordinate long-range structural changes in the L photointermediate of bacteriorhodopsin. *Biochemistry* **35**, 4063-4068
  55. Maeda, A., Kandori, H., Yamazaki, Y., Nishimura, S., Hatanaka, M., Chon, Y.-S., Sasaki, J., Needleman, R., and Lanyi, J.K. (1997) Intramembrane signaling mediated by hydrogen bonding of water and carboxyl groups in bacteriorhodopsin and rhodopsin. *J. Biochem.* **121**, 399-406